THEORETICAL REGIME DIAGRAMS FOR THERMALLY DRIVEN FLOWS IN A BETA-PLANE CHANNEL IN THE PRESENCE OF VARIABLE GRAVITY

J. E. Geisler and W. W. Fowlis

(NASA-CR-161580) NUMERICAL STUDY OF BAROCLINIC INSTABILITY Final Report, 1 Sep. - 30 Nov. 1979 (Miami Univ.) 17 p HC A02/MF A01 CSCL 04A

N80-33992

Unclas G3/46 28946

To appear as NASA Technical Paper

ABSTRACT

This paper examines the effect of a power law gravity field on baroclinic instability. We focus on the case of inverse fifth power gravity, since this is the power law produced when terrestrial gravity is simulated in spherical geometry by electrostatic means. We have obtained growth rates of unstable normal modes as a function of parameters of the problem by solving a second order differential equation numerically. Results are compared with those from an earlier study where gravity was a constant. The conclusion is that, over the range of parameter space explored here, there is no significant change in the character of theoretical regime diagrams if the vertically averaged gravity is used as parameter.

1. Introduction

It is generally agreed that the wavelike disturbances seen in rotating cylindrical geometry laboratory flow experiments are the result of baroclinic instability of axially-symmetric flow. This interpretation has been given a good theoretical basis by the study of Barcilon (1964), in which the eady model of baroclinic instability was used to obtain stability criteria for axially-symmetric flows. These criteria are in reasonable agreement with those observed in the laboratory for rotating anmilus flows.

In the earth's atmosphere baroclinic instability is also an important process for maintaining departures from axially-symmetric flow. It has long been felt that better simulation of atmospheric flow patterns or at least a better understanding of how and when baroclinic instability operates on the atmosphere could be achieved if laboratory rotating fluid experiments could be done in spherical geometry. Such experiments have not been realizeable because the dielectric body force for simulated radial gravity cannot be made large enough to dominate the effect of ambient terrestrial gravity in the laboratory. The low gravity environment aboard orbiting laboratories such as Spacelab, to be operational in the early 1980's, affords an opportunity for such an experiment.

In going from cylindrical geometry to spherical geometry in a rotating fluid experiment, one important new feature is the latitudinal variation of the local vertical component of rotation. As is well known, the effect of this on the dynamics of low frequency geophysical motions can be taken into account by β-plane geometry. As one of the first steps in developing a model for use in design of a Spacelab experiment, Geisler and Fowlis (1979) extended the work of Barcilon (1964) to a β-plane channel. The principal result of their study was to document the changes in the shape and location of the baroclinically unstable region of parameter space brought about by the latitudinal dependence of the vertical component of rotation.

One consequence of using a dielectric body force to simulate gravity is that the force field law is one of inverse fifth power (Hart, 1976). This must be taken into account in mathematical models of the proposed experiment and, moreover, is potentially troublesome because it does not simulate the inverse square of terrestrial gravity.

This paper describes the extension of the baroclinic instability model of Geisler and Fowlis (1979) to include an inverse fifth power law of gravity. The study shows that there is little difference between the stability information obtained from the two models provided gravity is replaced by its vertical average. This result supports conclusions earlier obtained for an annular geometry model by Giere and Fowlis (1979).

2. Formulation

Baroclinic instability in the presence of constant gravity was treated in Geisler and Fowlis (1979). In that paper we obtained growth rates and eigenfunctions for unstable modes in both the Charney and Eady models of baroclinic instability with and without Ekman damping at the boundaries. The normal modes were assumed to have the functional form

$$\psi(x,y,z,t) = \phi(z)\,\sin\left(\frac{n\pi y}{h}\right)\exp\left[ik(x-ct)\right] \tag{1}$$

where ψ is a stream function, h is the width of the channel and n is a positive integer. The equations solved there was

$$\left\{\frac{d^2}{dz^2} + \frac{N^2}{f_o^2}\left[\frac{\beta}{U-c} - \left(k^2 + \frac{n^2\pi^2}{h^2}\right)\right]\right\}\phi(z) = 0 \tag{2}$$

subject to the boundary conditions

$$\left\{ ik\left[(U - c)\frac{d}{dz} - \frac{dU}{dz}\right] \pm \frac{N^2}{2f_o}\left(\frac{2\nu}{f_o}\right)^{1/2}\left(k^2 + \frac{n^2\pi^2}{h^2}\right)\right\}\phi(z) = 0 \tag{3}$$

Where the plus sign applies at the upper boundary and the minus sign applies at the lower boundary.

In the above equations $U(z)$ is the basic state flow whose stability is being examined. As in Geisler and Fowlis (1979), we assume that the part of basic state temperature field $T(y,z)$ associated with $U(z)$ decreases linearly with y and the basic state temperature field $\langle T(z)\rangle$ associated with the static stability of the fluid increases linearly with z. These paremeters enter the problem through the thermal wind equation.

$$\frac{dU}{dz} = -\frac{g\alpha}{f_o}\left(\frac{\partial T}{\partial y}\right) \tag{4}$$

and through the definition of N^2

$$N^2 = g\alpha\left(\frac{d\langle T\rangle}{dz}\right) \tag{5}$$

Here T is the zonally averaged temperature, $\langle T\rangle$ is the area averaged temperature, α is the coefficient of thermal expansion of the fluid and g is gravity. In this paper we assign to g the variation.

$$g = \frac{g_o}{(1 + z/a)^p} \tag{6}$$

where p is an integer, a is the inner radius of the laboratory device and g_o is the value of g at $z = 0$. Integration of (4) upward from $z = 0$ (where we take $U = 0$) gives rhe basic state flow

$$U(z) = -\frac{ag_o\alpha}{f_o}\frac{\partial T}{\partial y}\left[\frac{1}{(p-1)}\left\{1 - (1+z/a)\right\}^{-p+1}\right] \tag{7}$$

If $p = 1$, integration of (4) gives the logarithmic flow

$$U(z) = -\frac{ag_o\alpha}{f_o}\frac{\partial T}{\partial y}\left[\ln(1+z/a)\right] \tag{8}$$

The stability of the flow given by equation (8) was examined by Giere and Fowlis (1979). In the present paper we examine the stability of the flow given by equation (7) with $p = 5$, that is, an inverse fifth power gravity.

In the case of $U(z)$ more general than the linear variation with z used in Geisler and Fowlis (1979), the parameter β in equation (1) should be replaced by

$$\beta - \frac{d}{dz}\left(\frac{f_o^2}{N^2}\frac{dU}{dz}\right) \tag{9}$$

However, as can be seen from equations (4) and (5), the factor g cancels out the correction to β then vanishes when $\partial T/\partial y$ and $d\langle T\rangle/dz$ are constant, as is the case here.

We introduce non-dimensional quantities denoted by a prime as follows:

$$x' = x/L \qquad k' = kL$$
$$y' = y/L \qquad U' = U/\Delta U \tag{10}$$
$$z' = z/d \qquad c' = U/\Delta U$$

Here L is an arbitrary horizontal length scale (taken to be 0.707a in Geisler and Fowlis, 1979)and dis the depth of the fluid. The quantity ΔU is $U(d)$, that is, the difference in the basic state flow between z = 0 and z = d. Equations (2) and (3) then become

$$\left[(U' - c')\left\{\frac{d^2}{dz'^2} - S\left(k'^2 + \frac{n^2\pi^2L^2}{h^2}\right)\right\} + B\right]\phi(z') = 0 \tag{11}$$

$$\left[(U' - c')\frac{d}{dz'} - \frac{dU'}{dz'} \pm \frac{S}{ik'R_o}\left(\frac{E}{2}\right)^{\frac{1}{2}}\left(k'^2 + \frac{n^2\pi^2L^2}{h^2}\right)\right]\phi(z') = 0 \tag{12}$$

The parameters in these equations are a static stability S, a β-parameter B, an Ekman number E and a thermal Rossby number R_o. They are defined as

$$S = \frac{N^2d^2}{f_o^2L^2} \quad ; \qquad B = \frac{\beta L^2}{\Delta U}S \tag{13}$$

$$E = \frac{u}{f_od^2} \quad ; \qquad R_o = \frac{\Delta U}{f_oL} \tag{14}$$

In the sequel, we refer to models with E = 0 in (12) as inviscid models. Equations (11) and (12), we refer to as the Charney model of baroclinic instability. The model obtained by setting B = 0 in (11), we refer to as the Eady model.

In the inviscid Eady model it is customary to display the behaviour of c_i (the imaginary part of the mode phase speed) in a diagram of $KS^{\frac{1}{2}}c'_i$ versus $KS^{\frac{1}{2}}$. Here S is given by (13) and

$$K = \left(k'^2 + \frac{n^2\pi^2L^2}{h^2} \right)^{\frac{1}{2}}, \tag{15}$$

Giere and Fowlis (1979) studied the unstable modes in the inviscid Eady model using the log profile basic state flow given by equation (8). They discovered that the curve changed very little over a wide range of the parameter d/a if $\overline{S}^{\frac{1}{2}}$ is used in the plot instead of $S^{\frac{1}{2}}$, where $\overline{S}$ is the value of S obtained from using in the definition of N^2 (see equation (6) and (13)) the vertically averaged value of g defined as

$$\overline{g} = g_o \int_o^1 \frac{dz'}{\left\{1 + \left(\frac{d}{a}\right)z'\right\}} \tag{16}$$

In the results reported in this paper we also use $\overline{S}$ rather than S in the graphical presentation.

3. Inviscid Model Results

All results presented here and in Section 4 were obtained by solving equation (11) subject to boundary conditions (12) using the numerical technique briefly described in Geisler and Fowlis (1979). As noted in Section 2, the difference between that and the present study is that we here use gravity which varies with radial distance according to the function

$$g = \frac{g_o}{\left|1 + \left(\frac{d}{a}\right) z'\right|^p} \tag{17}$$

where a is the inner radius and d the depth of the fluid.

As a cross check we first considered the case of p = 1 in the inviscid Eady model, a case for which analytic solutions were obtained by Giere and Fowlis (1979). We show in Figure (1) a plot of c_i' for runs with d/a = 0 (that is, constant g), d/a = 1, and d/a = 10. The figure confirms their result that inverse first power gravity has little effect provided the vertical average gravity is used for the plot. This agreement with their analytic result also indicates that the numerical routine is functioning correctly.

Figure (2) shows results for the inviscid Eady model when p = 5 (inverse fifth power gravity). Runs shown are those for d/a = 0, d/a =0.2 and d/a = 1. We have not gone beyond d/a = 1 because we anticipate that d/a will have to be <1 in any reasonable geophysical experiment. Figure (3) shows results when we go to the inviscid Charney model. Both Figure (2) and Figure (3) support the conclusion that, for the range of d/a of geophysical interest at least, such a plot is little affected by inverse fifth power gravity if the vertical average gravity is used.

4. Regime Diagrams

Superimposed contour diagrams of c_i for several values of zonal wave number k in the parameter space of S versus R_o^2/S^2E constitute a theoretical regime diagram. The construction of these diagrams for the Eady model and the Charney model was the subject of the paper by Geisler and Fowlis (1979). Figure (4) is taken from that paper and shows a theoretical regime diagram for the Eady model when d = h = L = 0.707a. (The parameter $\epsilon^2/\delta = R_o^2/S^2E$). The curve labelled (1) is the stability boundary for zonal wave number (1) disturbances, outside (to the left) of which c_i <0. The envelope of the curves shown in this figure obviously separates the region of parameter space where the flow is unstable from where the flow is stable and hence axially-symmetric. Geophysical experiments must be such that the unstable regime can exist in the apparatus, hence the utility of theoretical regime diagrams in experimental design studies.

To illustrate the results of our study of the effect of inverse fifth power gravity on theoretical regime diagrams, we have selected zonal wave number (3). Figure (5) shows contours of $KS^{-\frac{1}{2}}c_i'$ for this wave number in the Eady model when g is constant. The second case, where d/a = 0.5, is so close to this that it does not bear showing. Figure (6) shows the extreme (for a geophysical experiment) case for d/a = 1. Comparison with Figure 5 shows that the difference is rather small. We have run cases for other zonal wave numbers with the same result. The conclusion is that for d/a ≤ 1, the inverse fifth power gravity has only a small effect on the shape and location of the unstable regime provided vertically averaged g is used in drawing the diagram.

Figure (7) shows contours of $K\bar{S}^{-\frac{1}{2}}c_i'$ for zonal wave number (3) in the Charney model when g is constant. Here we adopt the value B = 2.35 used as a standard case in Geisler and Fowlis (1979). The case for d/a = 0.2 is again not much different and is not shown here. Figure (8) shows the case for d/a = 1. The change is somewhat greater than in the corresponding Eady model runs, the most notable change occurring in the region $\bar{S} \leq 0.1$. However, there is very little change in the leftward penetration of the nose located at about $\bar{S} = 0.2$. We have obtained similar results for other zonal wave numbers. We conclude that for d/a ≤ 1 the inverse fifth power gravity does not have significant affect on regime diagrams in either the Charney model or the Eady model provided $\bar{S}$ rather than S is used as the parameter.

References

Barcilon, V., 1964 : Role of Ekman layers in the stability of the symmetric regime obtained in a rotating annulus. J. Atmos. Sci., 21, 291-299.

Geisler, J. E. and W. W. Fowlis, 1979 : Theoretical regime diagrams for thermally driven flows in a beta-plane channel. J. Atmos. Sci., 36, 1530-1541.

Giere, A.C. and W. W.Fowlis, 1979 : Baroclinic instability with variable static stability. Submitted to Geophysical and Astrophysical Fluid Dynamics.

Hart, J. E., 1976 : Studies of earth simulation experiments. NASA Contractor Report NASA-CR2753

Figure Legends

Figure 1. Imaginary part of phase speed in the inviscid Eady model for the case of inverse first power gravity. Curves are labelled by the value of d/a. The dashed curve is the case of constant gravity.

Figure 2. Imaginary part of phase speed in the inviscid Eady model for the case of inverse fifth power gravity. Curves are labelled by the value of d/a. The dashed curve is the case of constant gravity.

Figure 3. Same as for Figure 2, but in the case of the inviscid Charney model.

Figure 4. Theoretical regime diagram for the Eady model with $d = h = a\cos\theta_o$ (from Geisler and Fowlis, 1979). The curves are stability boundaries labelled by zonal wave number.

Figure 5. Contours of imaginary part of phase speed $KS^{-2}c_i'$ in the Eady model with gravity constant.

Figure 6. Contours of imaginary part of phase speed $KS^{-1/2}c_i'$ in the Eady model with inverse fifth power gravity and $d/a = 1$.

Figure 7. Contours of imaginary part of phase speed $KS^{-1/2}c_i'$ in the Charney model with gravity constant.

Figure 8. Contours of imaginary part of phase speed $KS^{-1/2}c_i'$ in the Charney model with inverse fifth power gravity and $d/a = 1$.

Fig 1

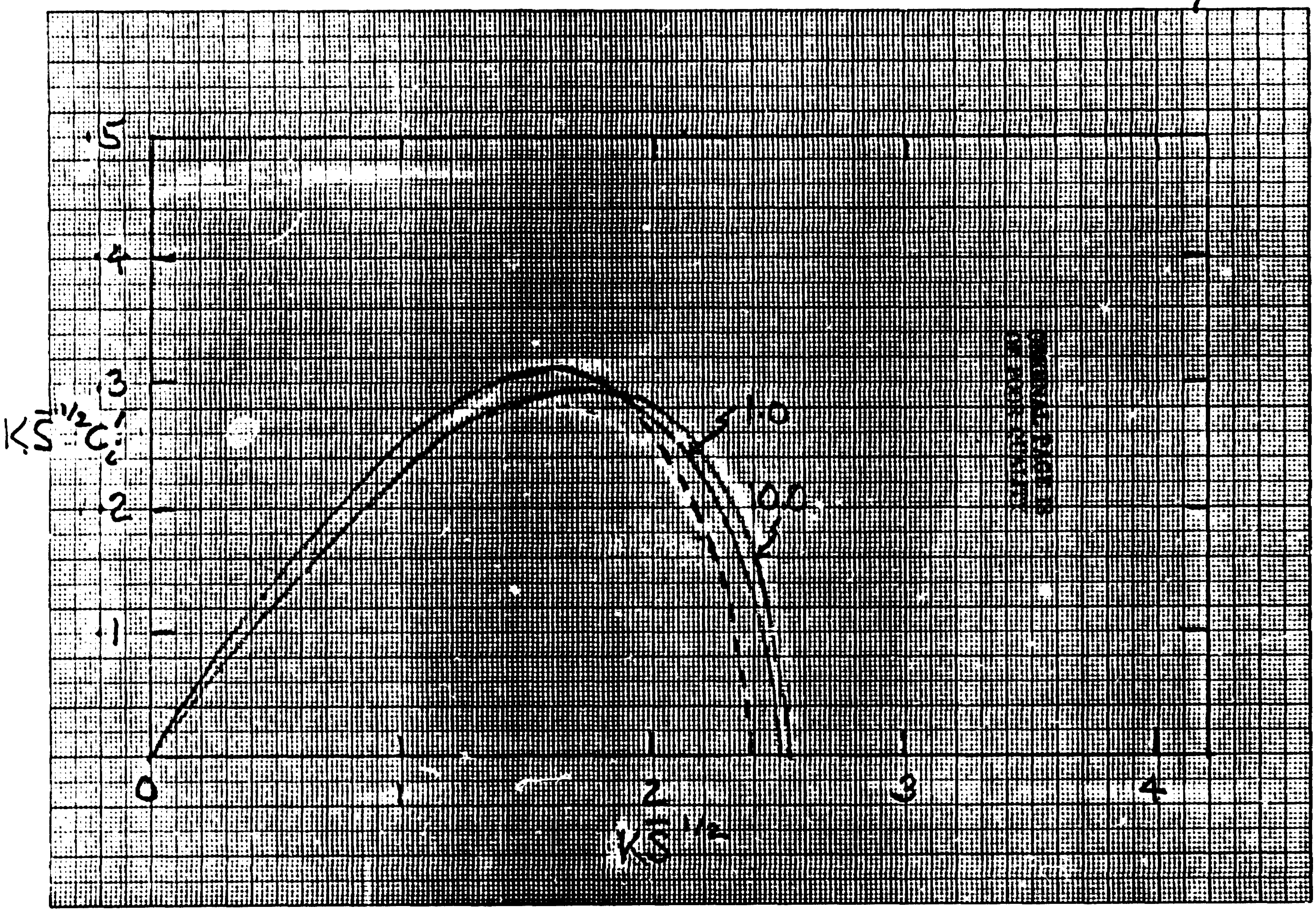

.5
.4
.3
.2
.1
$K\bar{S}^{1/2}C_c'$
0
1
2
3
4
$K\bar{S}^{1/2}$
1.0
0.0
ORIGINAL PAGE IS
OF POOR QUALITY

K•E 10 X 10 TO THE CENTIMETER 18 X 25 CM. KEUFFEL & ESSER CO. MADE IN U.S.A. 46 1517

Fig 2

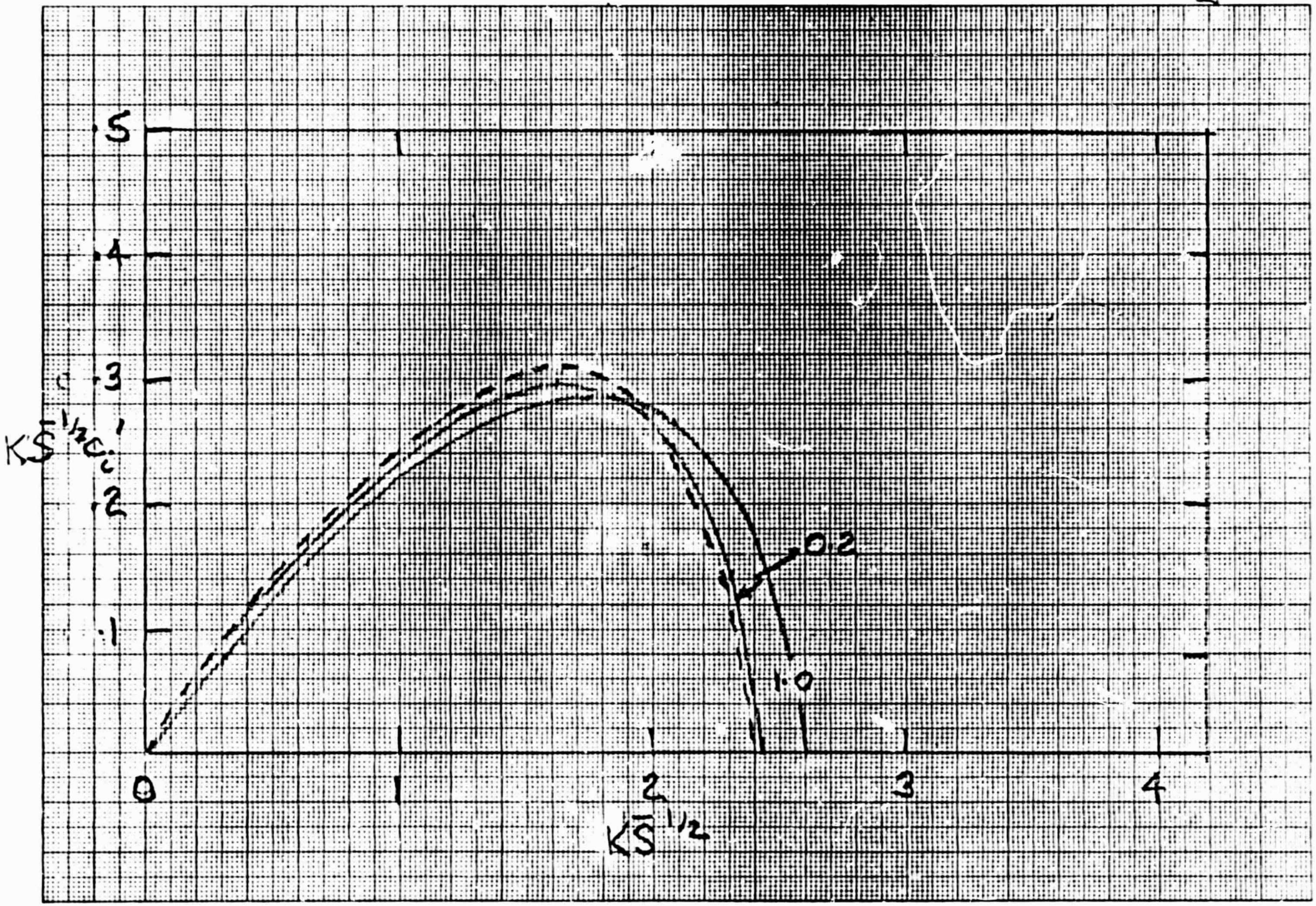

K•E 10 X 10 TO THE CENTIMETER 18 X 25 CM. KEUFFEL & ESSER CO. MADE IN U.S.A.

46 1517

Fig 3

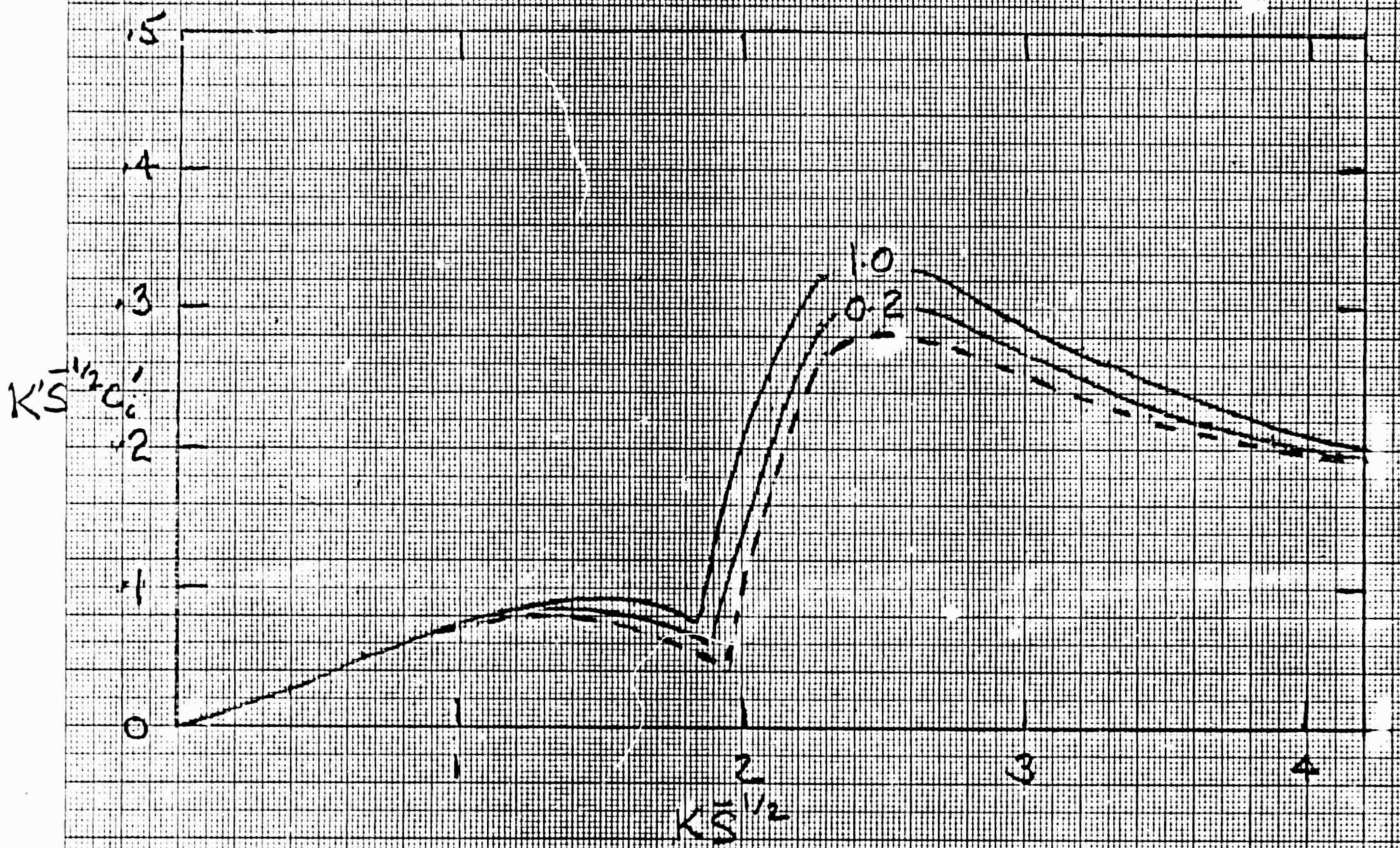

46 1517

Fig 4

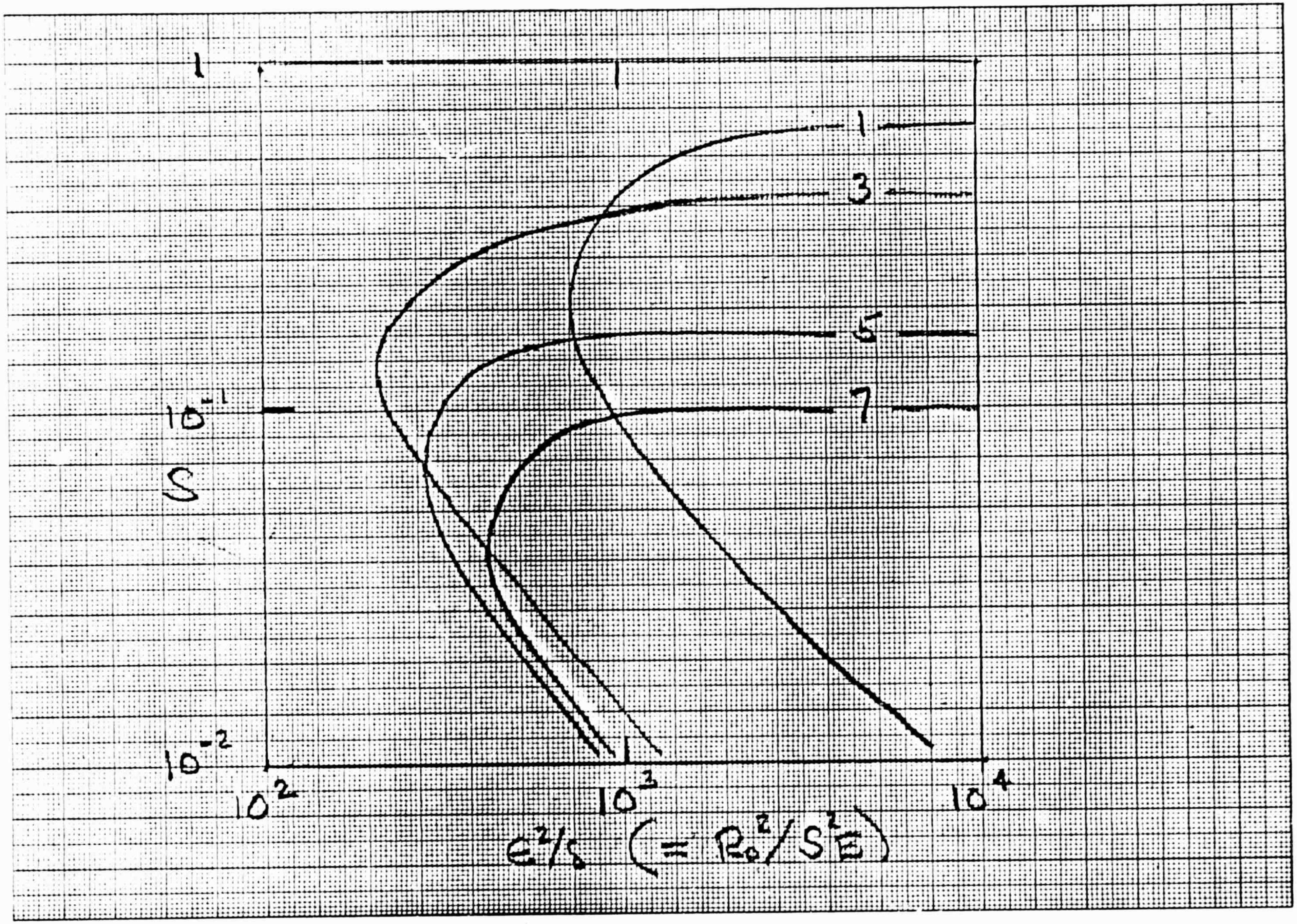

Fig 5

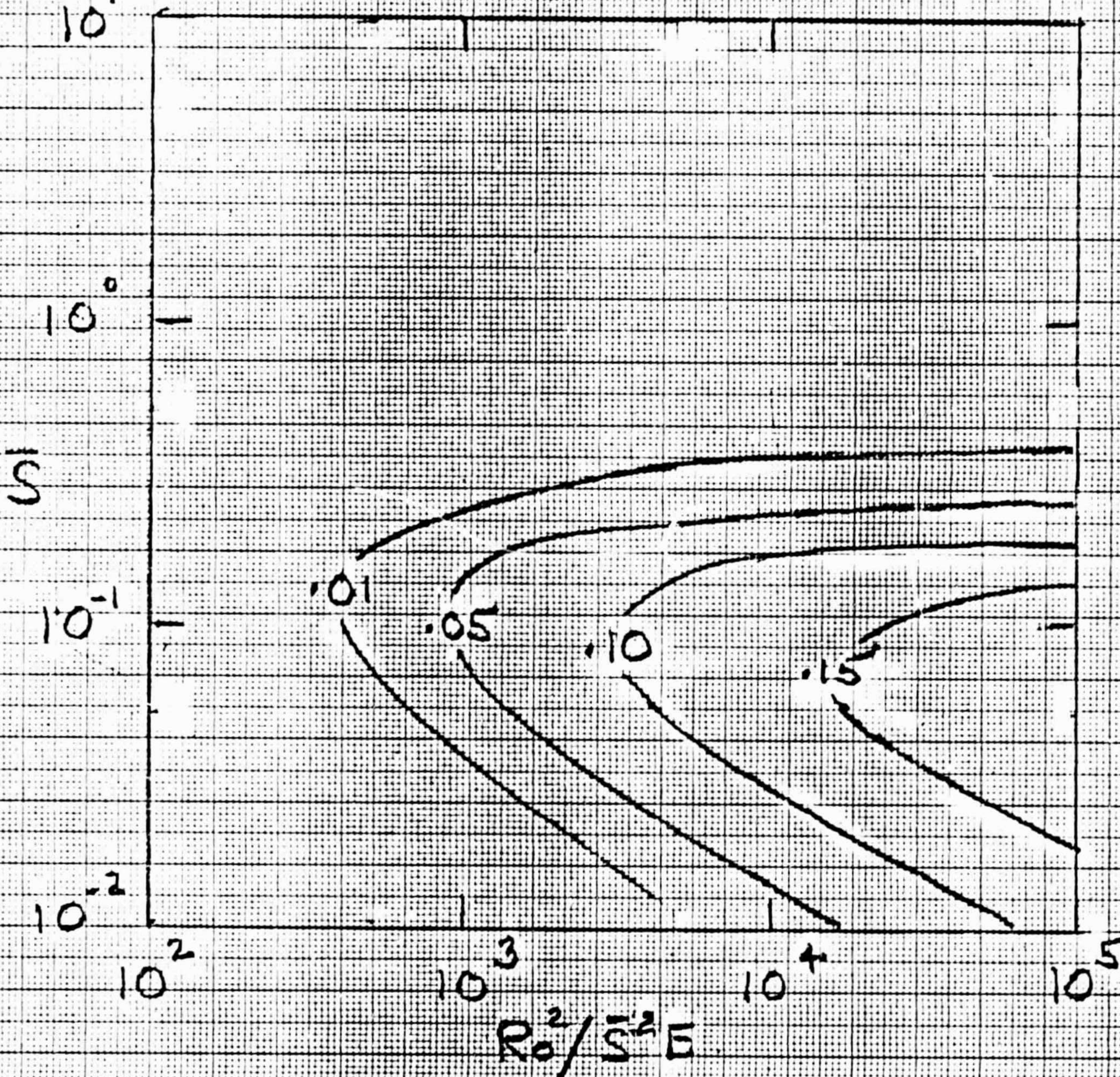

Fig 6

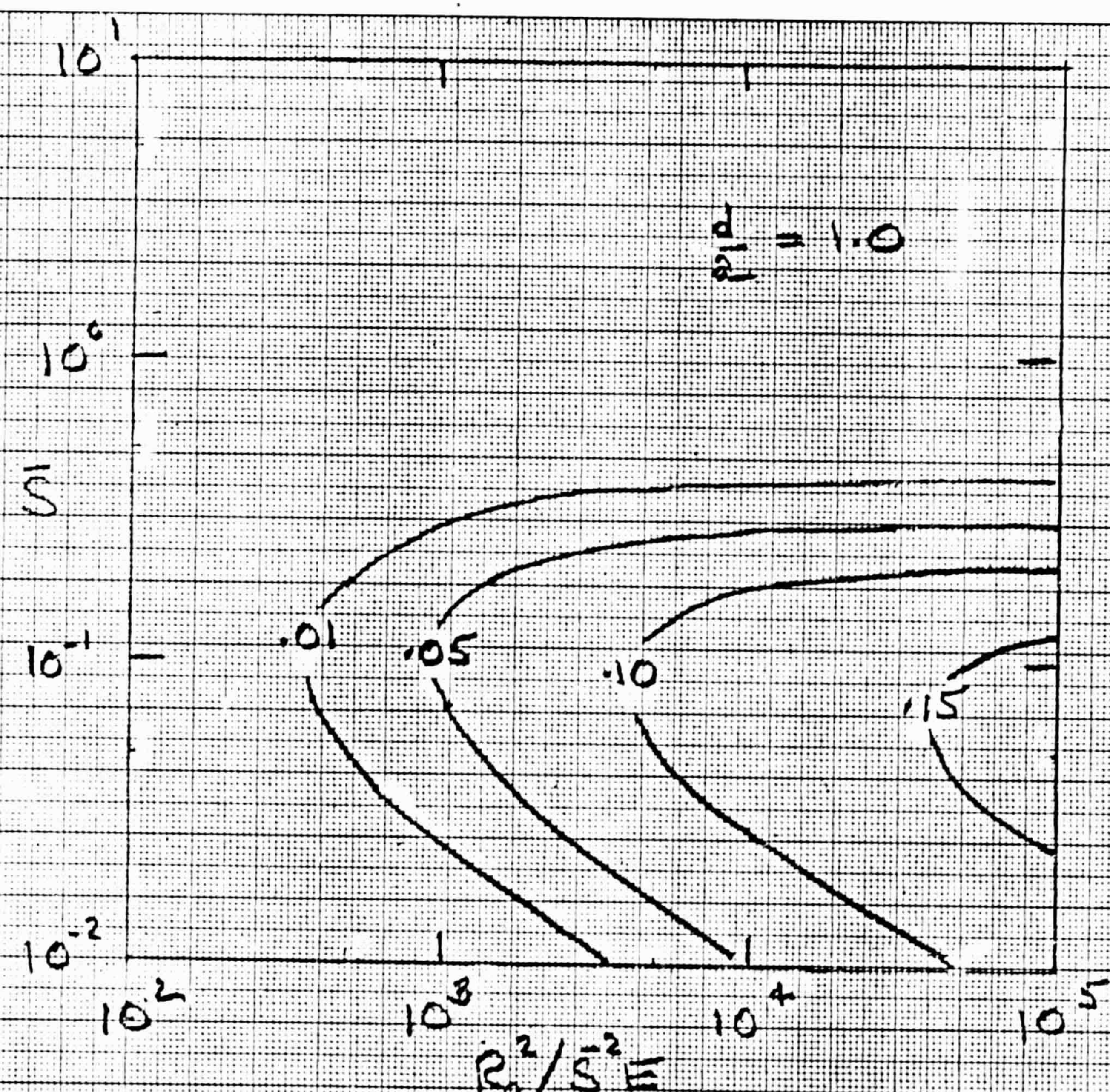

$\frac{d}{a} = 1.0$
.01
.05
.10
.15
10^{1}
10^{0}
$\bar{S}$
10^{-1}
10^{-2}
10^{2}
10^{3}
10^{4}
10^{5}
$R_0^2/\bar{S}^2 E$

K•E 10 X 10 TO THE CENTIMETER 18 X 25 CM. KEUFFEL & ESSER CO. MADE IN U.S.A. 46 1517

Fig 7

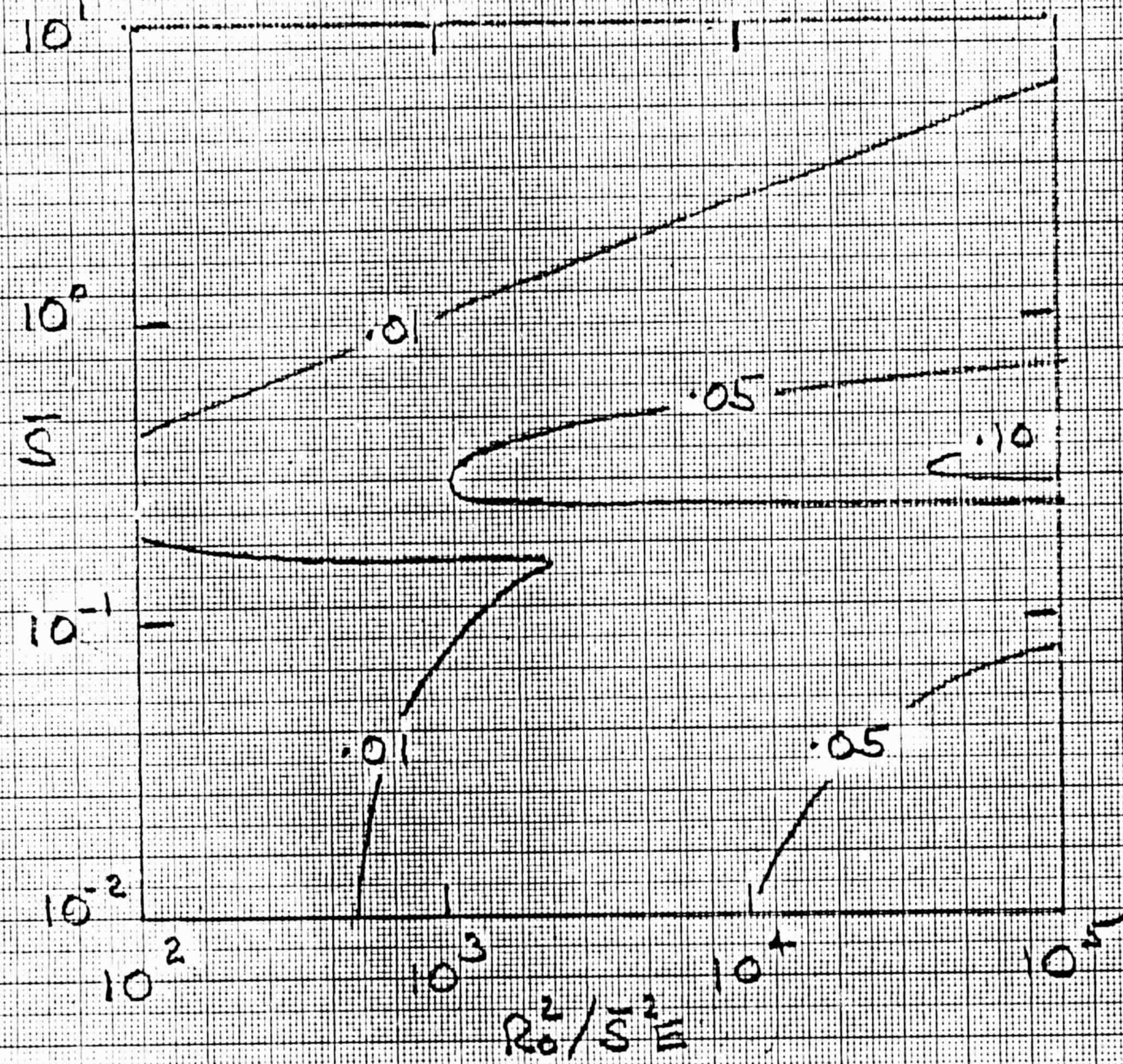

46 1517

Fig 8

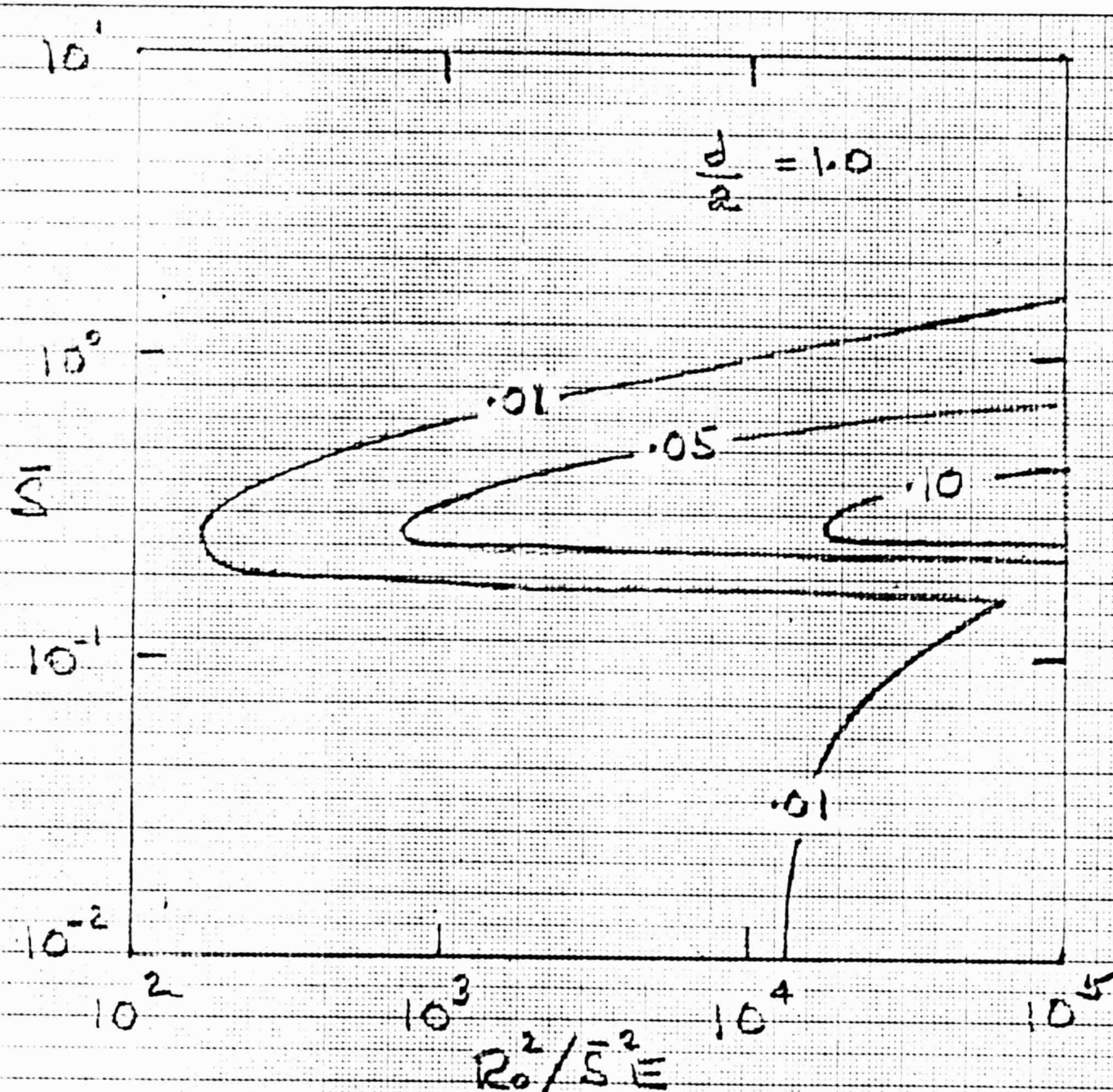
$\frac{d}{a} = 1.0$
.01
.05
.10
.01
10^1
10^0
$\bar{S}$
10^{-1}
10^{-2}
10^2
10^3
10^4
10^5
$R_o^2/\bar{S}^2 E$